Acta Oceanol. Sin., 2024, Vol. 43, No. 12, P. 47–57
https://doi.org/10.1007/s13131-024-2417-5
http://www.aosocean.com
E-mail: ocean2@hyxb.org.cn

A preliminary study on dissolved iodine in the northern South China Sea Shelf

Jianrong Lin[1]*

[1] Key Laboratory of Estuarine Ecological Security and Environmental Health of Fujian Province University (Xiamen University Tan Kah Kee College), Zhangzhou 363105, China

Received 20 February 2024; accepted 7 May 2024

Abstract

We investigated dissolved iodine species in seawater from the northern South China Sea Shelf. Iodide concentrations were determined by cathodic stripping square wave voltammetry, and iodate was measured by spectrophotometry. Dissolved organic iodine (DOI) was measured with reference to reduced iodide. R-TDI (R-*X* or rationalized-*X* is the concentration of *X* normalized to a salinity of 35, TDI represents total dissolved iodine) was in the range of 0.43–0.46 μmol/L, showing a relatively conservative behavior, while iodate, iodide, and DOI showed non-conservative behaviors. Distribution characteristics in the surface waters showed R-iodate values in the 0.28–0.32 μmol/L range and an offshore>inshore trend, while R-iodide was in the 0.11–0.19 μmol/L range and R-DOI in the 0–0.07 μmol/L range, reflecting an inshore>offshore trend for both. The vertical distribution showed the highest R-iodide concentrations in the surface waters and decreased values with depth, reaching less than 0.01 μmol/L at depths>200 m. R-iodate increased with depth with a measured peak value of 0.43 μmol/L. Seawater with high iodate/iodide ratio (up to 2.9) was found in the central upwelling region and gradually decreased to 2.0 far from this center. The relationship between R-iodide and R-iodate among all samples followed the 1:1 relationship with a slope slightly less than 1, indicating that the conversion between iodate and iodide species could not account for the observed changes. This finding also suggests that DOI may be an important participant in the mass balance. A box model was applied to calculate the input and output of iodine species, and the result showed that approximately 8% of iodate (1.50×10^8 mol/a) imported to the shelf sea was reduced. Concomitantly, the amount of iodide and DOI produced in the shelf amounted to 1.07×10^8 mol/a, roughly 14% higher than the input iodide.

Key words: total dissolved iodine, iodate, iodide, dissolved organic iodine, northern South China Sea Shelf

Citation: Lin Jianrong. 2024. A preliminary study on dissolved iodine in the northern South China Sea Shelf. Acta Oceanologica Sinica, 43(12): 47–57, doi: 10.1007/s13131-024-2417-5

1 Introduction

In the ocean, iodate (IO_3^-, oxidized form), iodide (I^-, reduced form), and dissolved organic iodine (DOI) are the dominant iodine species, with an estimated total concentration of 0.45 μmol/L (Tsunogai and Henmi, 1971; Wong, 1991; Lee Chen, 2005; MacKeown et al., 2022; Lin, 2023). Thermodynamically, iodate is the favored form of iodine and the overwhelmingly dominant form below the oceanic mixed layer in oxygenated seawater. The existence of DOI in seawater was first reported by Truesdale (1975), and its significance has been highlighted, particularly in coastal waters (Wong and Cheng, 2001a, 2008; Lin, 2023). Research has revealed that different iodine species can be converted into one another in continental shelf seas (Wong and Zhang, 2003a; Wong et al., 2004; Wong and Cheng, 2008; Chance et al., 2010; Zhou et al., 2017; Carrano et al., 2020; MacKeown et al., 2022; Lin, 2023; Shaikh et al., 2023). For example, in the Antarctic shelf sea area, the concentration of iodide increases with increasing chlorophyll *a* (Chl *a*) concentration (Chance et al., 2010). In general, iodine speciation changes are much more pronounced in shelf waters than in the open ocean (Truesdale, 1994; Truesdale and Jones, 2000; Truesdale and Upstill-Goddard, 2003; Wong and Zhang, 2003a; Truesdale et al., 2003; Wong et al., 2004; Chance et al., 2010; Moriyasu et al., 2020; MacKeown et al., 2022; Lin, 2023; Shaikh et al., 2023). In addition to biological factors, iodine in shelf waters is controlled by physical processes, such as upwelling and internal waves (Wong et al., 2004; Chance et al., 2010; Moriyasu et al., 2020; MacKeown et al., 2022). In the euphotic layer, iodate increases and iodide decreases with depth, and $[IO_3^-]/[I^-]$ increases with water depth. The $[IO_3^-]$, $[I^-]$, and $[IO_3^-]/[I^-]$ molar ratio characteristics of upwelled waters are distinct from those of surface waters. Hence, iodine can be used as a tracer. As a tracer, iodine offers advantages over temperature and salinity because the efficacy of temperature and salinity can be seriously limited in shelf environments. This limitation arises because coastal waters may also have the same signatures. Furthermore, temperature can be modified by heat exchange between the sea surface and the atmosphere (Wong et al., 2004). Similarly, iodine can be used to trace internal waves.

Iodide produced in the shelf sea may also be imported into the open ocean (Wong, 1995; Wong and Zhang, 2003a; Wong et al., 2004; Wong and Cheng, 2008). For East China Sea and South Atlantic Bay, the annual net output of iodide generated by iodate is around 1.0×10^9 mol/a and 1.8×10^9 mol/a, respectively, while other studies show no evidence of conversion from iodate to iodide (Truesdale, 1978, 1994; Truesdale and Jones, 2000), indicating further the need for more studies.

Foundation item: The Zhangzhou National Science Foundation of Fujian under contract No.JJ2020J29.
*Corresponding author, E-mail: jrlin@xmu.edu.cn

In this study, the distribution of iodine species in the northern South China Sea was studied, and a box model was used to calculate the import and export of the iodine species.

2 Study area and methods

2.1 *Study area*

The South China Sea is located in the region bound within 4°–23°N, 105°–121°E and has an estimated area of 3.56×10^6 km^2 (Wong et al., 2007). Owing to the influence of southwest winds, the northern shelf area of the South China Sea can experience wind-driven upwelling in summer, such as in East Guangdong (Wu and Li, 2003). The northern Luzon Strait is the main channel connecting the South China Sea and the West Pacific. The deep water of the West Pacific enters the South China Sea through the Luzon Strait. The residence time of deep water is about 30 years. Water balance with the input of deep water is mainly realized through the output of middle layer water (Wong et al., 2007). The Research Center for Environmental Changes (RCEC) at Academia Sinica organized the South China Sea Shelf Sea OR1-CR929 cruise from June 3 to 12, 2010. Our report covers four sections from east to west, labeled T1, T2, T3, and T4, each consisting of 12–15 stations (Fig. 1).

We divided the sea area into four areas according to bathymetry: inner-shelf (⩽40 m), mid-shelf (40–90 m), outer-shelf (90–120 m), and open SCS (>120 m). The depth of the outer continental shelf is taken to be 120 m in this research. The water area and volume of each part of the continental shelf are listed in Table 1.

2.2 *Sampling methods*

The sampling bottles used were made from high-density polyethylene or polypropylene that needed to be pretreated before sampling. The steps were as follows: (1) soaking in reverse osmosis water for at least 24 h, (2) washing with detergent (2% micro) (Cole Parmer Company) and then rinsing with RO water, (3) washing with RO water after soaking in 10% HCl for 24 h, and (4) drying in a clean room. The filter membrane was soaked in 0.5 mol/L HCl solution for 12 h, washed with Milli-Q water to neutral, and dried in a clean room. After sampling, the bottle cap was tightened and immediately stored in a –20℃ refrigerator. The cap was confirmed to still be tight after several hours when the sample was frozen.

2.3 *Measuring methods*

Iodide was determined by cathodic stripping square wave voltammetry, which has a precision of ±5%. At –0.15 V (relative to standard calomel) potential, Hg initially lost electrons, and then iodine was deposited onto the suspended mercury electrode in the form of Hg_2I_2 for a certain time. The addition of Triton X-100 to the solution resulted in a significant increase in peak current, and the peak height was positively correlated with the iodide concentration. Quantitative analysis was carried out by adding different iodide concentrations in solution. Dissolved oxygen was removed by aeration with high-purity argon. Sulfite was added to the solution to remove oxygen quickly. Iodate was measured by a spectrophotometric method with a Shimadzu UV1700 spectrophotometer, which has ±3% precision. DOI was measured as reduced iodide according to the method developed by (Wong and Cheng, 1998).

Nitrate and Chl *a* data were supplied by RCEC. Longitudes,

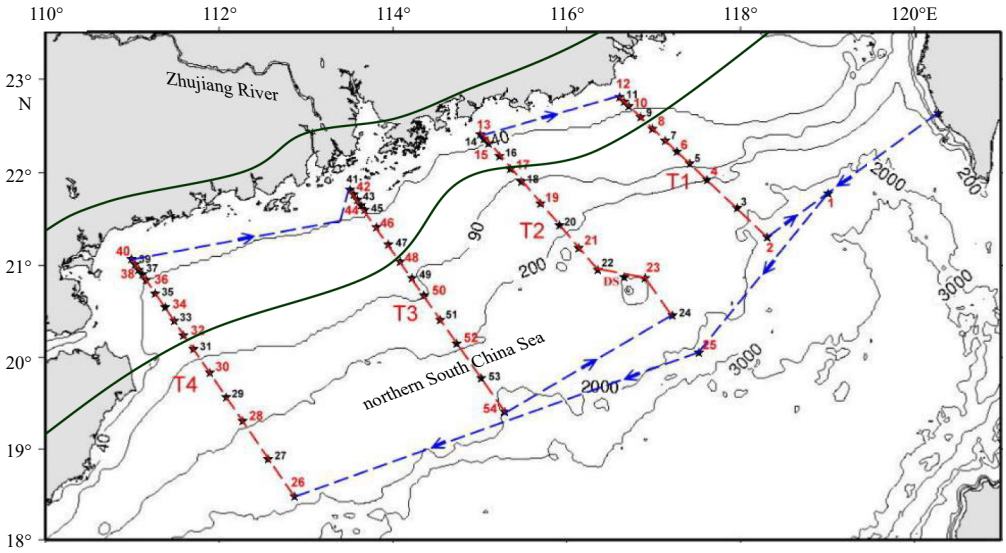

Fig. 1. Sampling sites in the northern South China Sea in June 2010 from east to west: T1, T2, T3, and T4.

Table 1. Sub-areas of the northern South China Sea Shelf

Sub-area	Bathymetry/m	Water depth/m	Area/km^2	Volume/km^3
Inner shelf	0 < bathymetry ⩽ 40	0 – 40	64 981	1 124
Middle shelf	40 < bathymetry ⩽ 90	0 – 40	67 763	2 711
		40 – 90	67 783	1 509
Outer shelf	90 < bathymetry ⩽ 120	0 – 40	28 319	1 133
		40 – 120	28 319	1 597
Total	Water depth ⩽ 120		161 083	8 074

latitudes, salinity, and temperature were received with a GPS receiver in real time and recorded with cruise CTD data. The precision of longitude and latitude was ±0.000 01° accurate, salinity precision was ±0.01, and temperature precision was ±0.001℃.

3 Results

3.1 *Surface and vertical distribution of temperature and salinity*

Figure 2 shows the surface temperature and salinity. Figures 3 and 4 illustrate the sector and vertical distribution of temperature, salinity, Chl *a*, and nitrate for each section, respectively.

In general, surface temperature and salinity increased from the inner to the outer shelf (Figs 2 and 3b1–b4); in the inner and outer shelves, the temperature and salinity increased from about 26℃ to 26.5℃ and from 27 to 28, respectively. The freshwater signal in the west shelf (Figs 2 and 3b4) is characterized by higher temperature (~28℃) and lower salinity (~24.5) than surrounding waters. In a typical summer, the temperature and salinity of shelf waters are greatly affected by freshwater input from the Zhujiang River (Callahan et al., 2004; Cai et al., 2004).

Upwelling is observed in the eastern part of the inner shelf, which is characterized by lower temperature and higher salinity than surrounding waters. The average surface salinity is about 34.2 (non-upwelling < 33.6) and the temperature is around 24.6℃ (non-upwelling > 25.8℃) (Figs 2 and 3b2). Although temperature can serve as a good tracer in the central upwelling area, this is only true during periods of pronounced wind-driven upwelling.

The concentration of upwelling nitrate is comparable to that in other continental shelf sea areas. The South China Sea is an oligotrophic sea. The nitrate levels in the shallow water bodies above the continental shelf were near or below the detection lim-

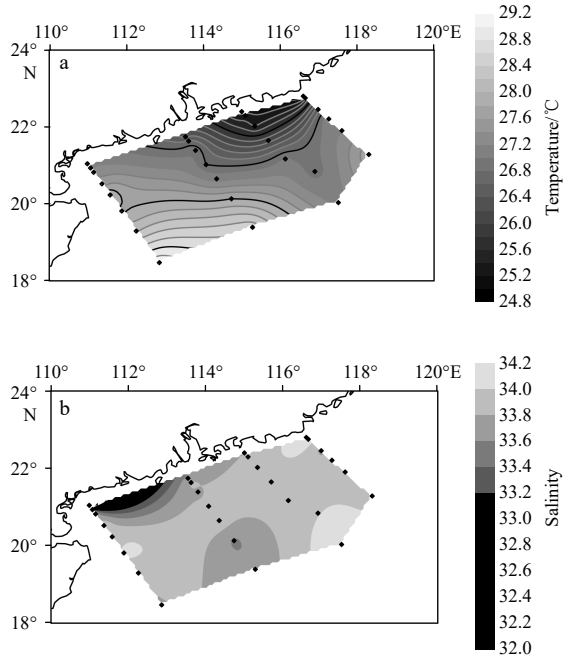

Fig. 2. Surface distribution of temperature and salinity in June 2010 cruise.

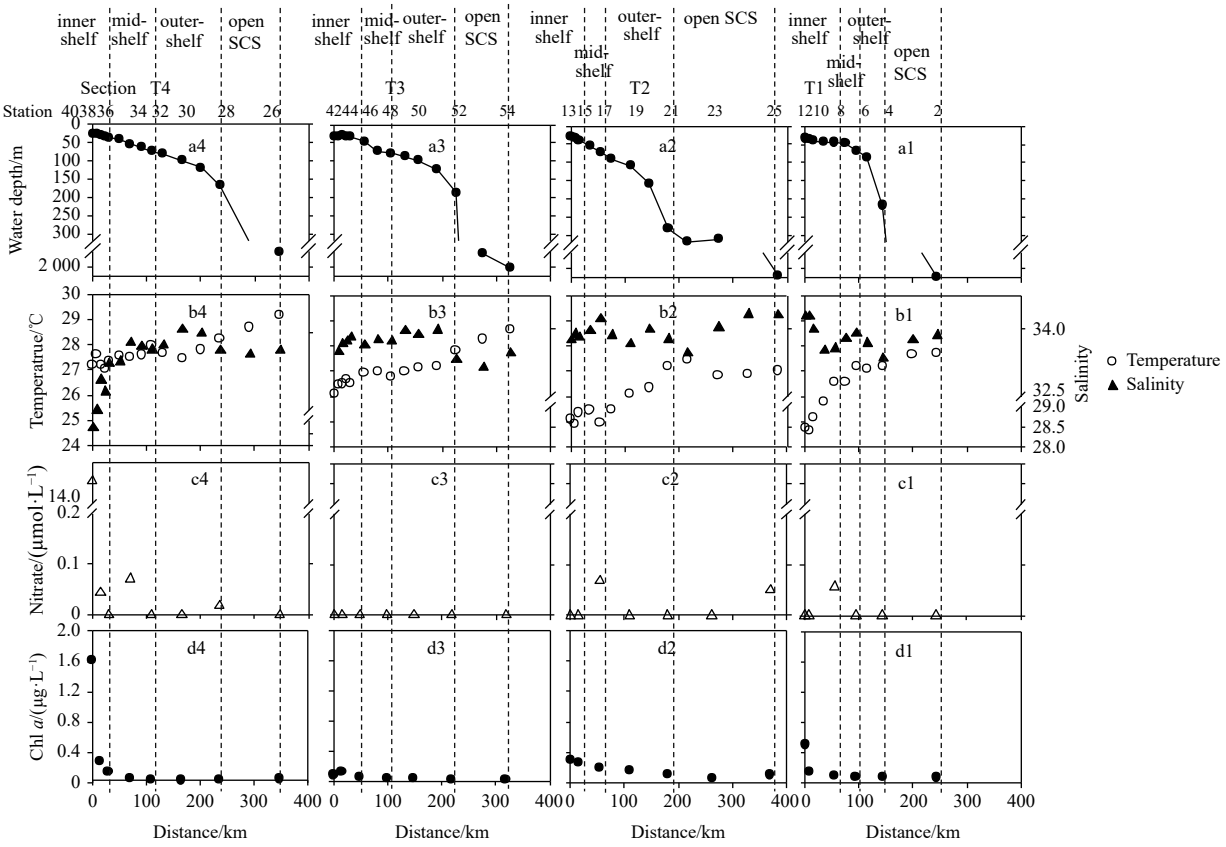

Fig. 3. Sector distribution of water depth (a1–a4), temperature and salinity (b1–b4), nitrate concentration (c1–c4) and Chl *a* concentration (d1–d4) in the northern South China Sea Shelf-sea surface water in June 2010. The stations between the dashed line represent the inner shelf, middle shelf, outer shelf, and open SCS, respectively.

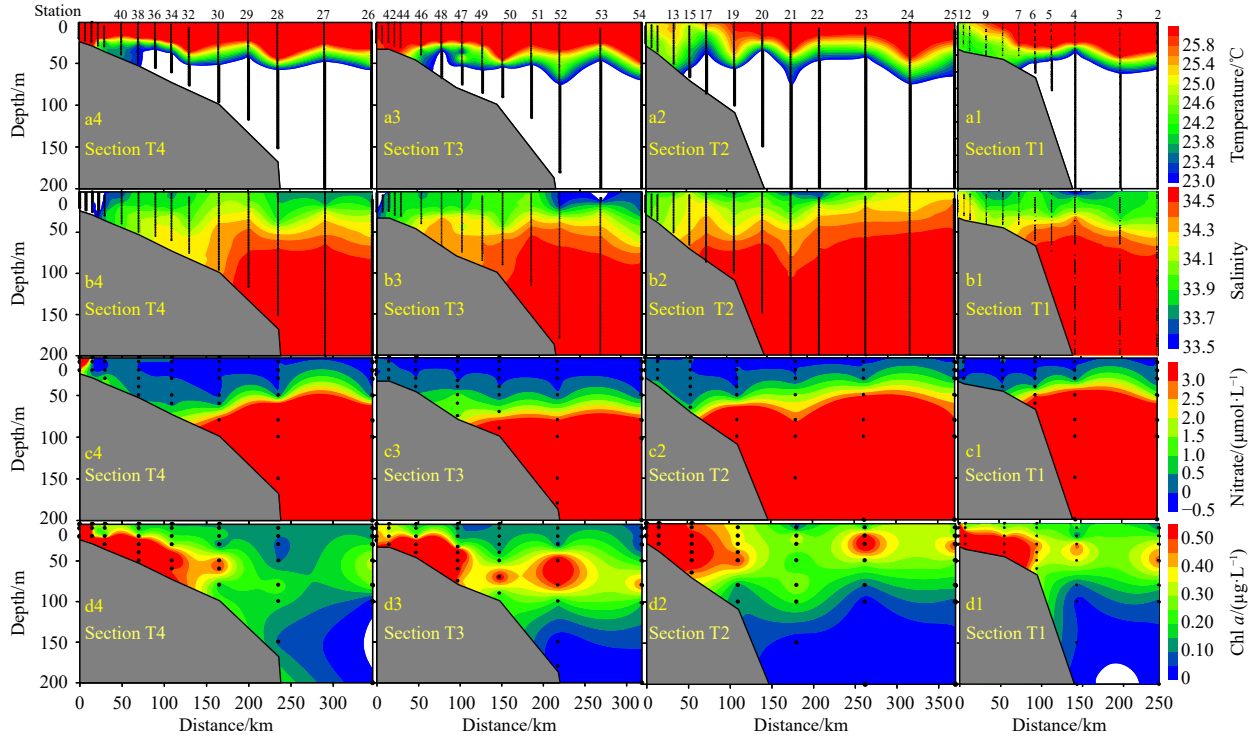

Fig. 4. Vertical distribution of temperature (a1–a4), salinity (b1–b4), nitrate concentration (c1–c4), and Chl *a* concentration (d1–d4) of Sections T1–T4 in the northern South China Sea in June 2010.

it during the investigation period (Figs 3c1–c4). This implies that upwelling that sourced water from shallow depths did not cause an increase in surface nutrients.

The temperature, salinity, nutrients, and chlorophyll of each section reflect the oceanographic setting of each site (Fig. 4). For example, along Section T2, Stations 22 and 23 (near Dongsha Islands), strong internal waves are formed due to the bathymetry, resulting in deep water upwelling (Fig. 4b2). At Stations 22 and 23, from depths of 20–120 m, the average temperature and salinity are (21.13 ± 3.92)℃ and (21.05 ± 3.47)℃, 34.47 ± 0.14 and 34.52 ± 0.13, respectively. At the nearby Stations (21, 24), the temperature and salinity progressed from (22.93 ± 2.38)℃ and (22.56 ± 3.38)℃, 34.33 ± 0.18 and 34.50 ± 0.12, respectively. Although the difference in salinity is not significant, the average temperature difference between them is as high as 1.8℃. Lower-temperature water bodies are caused by the rise of deep water. Second, there is enhanced water column mixing near the shore; in Station 17, the surface salinity exceeds 34.2, which is about 0.6 higher than the average of the inland shelf. At the same time, the temperature drops to about 24.6℃ (Figs 3b2, 4a2 and 4b2).

The most obvious feature of Section T3 is the low salinity of surface water, to a depth of 20 m, at Stations 52–54 (Fig. 4b3). The average salinity of the three stations below 20 m is 33.633 ± 0.107, while at the adjacent Station 25, the average salinity of the station below 20 m is 34.375 ± 0.071, a difference of more than 0.7. This discrepancy may be caused by precipitation.

The most notable feature of Section T4 is that several stations on the inland shelf are affected by freshwater input (Figs 4a4, b4, c4 and d4). The lowest salinity value appeared at Station 40. A front appeared at Stations 39 and 40: within a range of 7.6 km, salinity increased from 28.7 to above 33. This is the largest salinity variation observed during the voyage, which may be attributed to the westward transport of Zhujiang River freshwater. Previous studies have found that about one-third of Zhujiang River freshwater moves westward in summer (Pan et al., 2006; Su, 2004). High nitrate and chlorophyll concentrations reaching 14.9 μmol/L and 2.89 μg/L, respectively, are found, likely influenced by Zhujiang River water input. Nitrate concentration can reach >100 times the value of continental shelf water (Dai et al., 2008). A notable feature of Section T4 is that the inner shelf area shows high nitrate and chlorophyll values due to the impact of freshwater input, with the highest values of 14 μmol/L and 1.6 μg/L (Figs 3c1 and d1), respectively.

In general, temperature and salinity increase from the continental shelf toward the deep ocean basin, while nutrient and chlorophyll concentrations rapidly decrease. This represented a typical summer when the northern South China Sea is greatly affected by freshwater input from Zhujiang River. Moreover, the shelf mixed layer is generally in an oligotrophic state, which is consistent with the results of Yuan (2005).

3.2 *DI in the northern South China Sea*

The variation of R-TDI and R-total inorganic iodine (TII) in the continental shelf area is not significant, only about (0.43 ± 0.03) μmol/L (Figs 5a1–a4), indicating that the proportion of exchanging species from dissolved to other phases is very small. Other external input sources, such as atmospheric deposition, river water, or sediment interstitial water, can also be ignored.

Contrary to the R-TDI distribution, the changes in surface IO_3^- and I^- concentrations are significant (Figs 5b1–b4). The surface IO_3^- (R-IO_3^-) shows a trend of low near shore and high far shore, with IO_3^- ranging from 0.257 μmol/L to 0.319 μmol/L. On the contrary, the surface I^- (R-I^-) shows a trend of low far shore and low near shore, with I^- ranging from 0.11 μmol/L to 0.21 μmol/L. I^- variation is greater than that of the continental shelf I^- along the coast of the United States (Wong and Zhang,

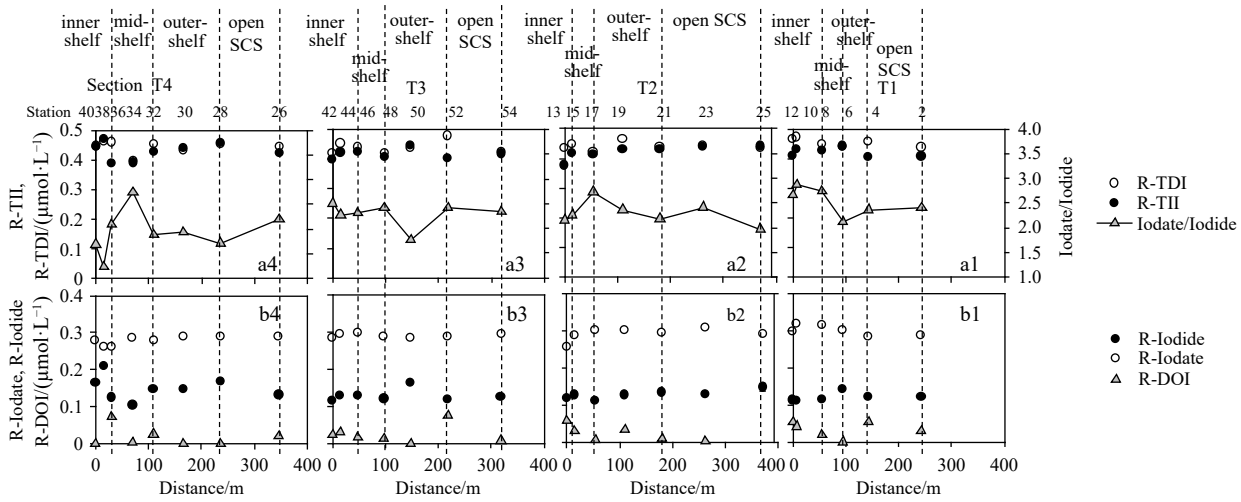

Fig. 5. Sector distribution of R-Iodide, R-Iodate, R-DOI, and R-TDI in four sections in the cruise conducted in June. Stations between the dashed line represent inner shelf, middle shelf, outer shelf, and open SCS, respectively. R-*X* represents the concentration that has been normalized to salinity 35.

1992; Wong, 1995).

Iodide is inversely correlated with iodate, and the variation in the ratio of IO_3^-/I^- is also significant (Figs 5a1–a4). The minimum of 1.3 appears at the area of freshwater input, while the maximum of 2.9 appears at the upwelling area.

The vertical distribution of the mixing layer is similar to that of the surface layer, with I^- concentration increasing while IO_3^- decreases from the outer shelf to the inner shelf. Below the mixing layer, R-TDI exhibits a conservative behavior (Fig. 6). From the open SCS (40–120 m), outer shelf (40–120 m), middle shelf (40–90 m) to inner shelf (0–40 m), the average concentration of R-IO_3^- decreases from 0.356 μmol/L to 0.283 μmol/L, while R-I^- and R-DOI increase from 0.065 μmol/L to 0.138 μmol/L and from 0.018 μmol/L to 0.025 μmol/L, respectively. In particular, during the transport of seawater from the outer shelf to the inner shelf, dissolved iodine changes due to enhanced biological effects.

The results are similar to those of the shelf sea of England and East China Sea (Truesdale and Jones, 2000; Wong and Zhang, 2003a) but much smaller than that of the continental shelf sea in the southeastern United States, where the proportion of IO_3^- converted into other species is about 60%–80% (Wong and Zhang, 1992; Wong, 1995). This is the main difference between middle/high and low-latitude shelf marginal seas (Wong and Zhang, 1992; Wong, 1995; Truesdale and Jones, 2000; Wong and Zhang, 2003a).

The temperature, salinity, and dissolved iodine profiles at four deep-water stations on the South China Sea slope are shown in Fig. 7. The average concentrations of R-TDI in the mixed layer (0–40 m) or euphotic layer (40–130 m) are (0.437 ± 0.016) μmol/L and (0.442 ± 0.020) μmol/L, respectively. At 2 000 m depth, the value is (0.465 ± 0.010) μmol/L. Overall, the R-TDI only has a slight change in all depths.

The concentration of dissolved iodine in different forms varies greatly with depth. The iodide in the mixed layer (0–40 m) is (0.127 ± 0.015) μmol/L (Table 2), which decreases rapidly with increasing depth. When the depth is >200 m, the iodide falls below the detection limit. The iodate in the mixed layer is (0.296 ± 0.011) μmol/L, which increases to above (0.422 ± 0.005) μmol/L when the depth >200 m, slowly increasing with depth and remaining almost constant below 1 000 m. These results are similar to the results of open oceans such as the Atlantic and Pacific (Tsunogai and Henmi, 1971; Wong, 1991; Wong and Cheng, 2001a), where iodine exchange mainly occurs within the euphotic layer.

4 Discussion

4.1 *Tracing upwelling*

Upwelling promotes high IO_3^- and low I^- concentrations, leading to high IO_3^-/I^- ratios. Therefore, iodine can be used to study upwelling. Compared with iodine systems, salinity and temperature have the following limitations: after the upwelling enters the surface, the sea surface temperature in the upwelling area and other sea areas will quickly converge due to the heat exchange between the sea surface and the atmosphere. Surface water salinity is significantly different from upwelled water. When the salinity of the surface water and the upswelled water is similar, it is difficult to use salinity as an indicator of upwelling (Wong and Zhang, 2003a; Wong et al., 2004). Choosing IO_3^-/I^- ratios can overcome these shortcomings; it is not only a supplement to traditional upwelling indicators but can also be used as the primary indicator when temperature and salinity are insensitive to upwelling.

The IO_3^-/I^- ratios of the mixed layer in the northern shelf of the South China Sea during the cruise was in the range of 1.2–3 (the uncertainty of the ratio is ~0.05) (Table 2). In the western shelf due to freshwater input, which resulted in the lowest surface IO_3^-/I^- ratio reaching 1.2, the ratio range in most sea areas was above 2, with the highest ratio of 3.0 occurring in the upwelling center of the eastern shelf, similar to the research results in the East China Sea (Wong and Zhang, 2003a). The ratio of IO_3^-/I^- can provide information on where water rises from. The ratio of IO_3^-/I^- at 40 m and 50 m is 3 and 3.6, respectively, and the average value of IO_3^-/I^- at 0–40 m is about 2.5. In addition, the continental shelf area is 5.9, while the ratio outside the shelf is around 10 (Table 2). Therefore, it is reasonable to believe that the upwelling in the South China Sea inner shelf should be around 40 m.

4.2 *Iodine species conversion in the northern South China Sea*

Analyzing the distribution of iodine at deep-water stations in the South China Sea can help scholars understand the similarit-

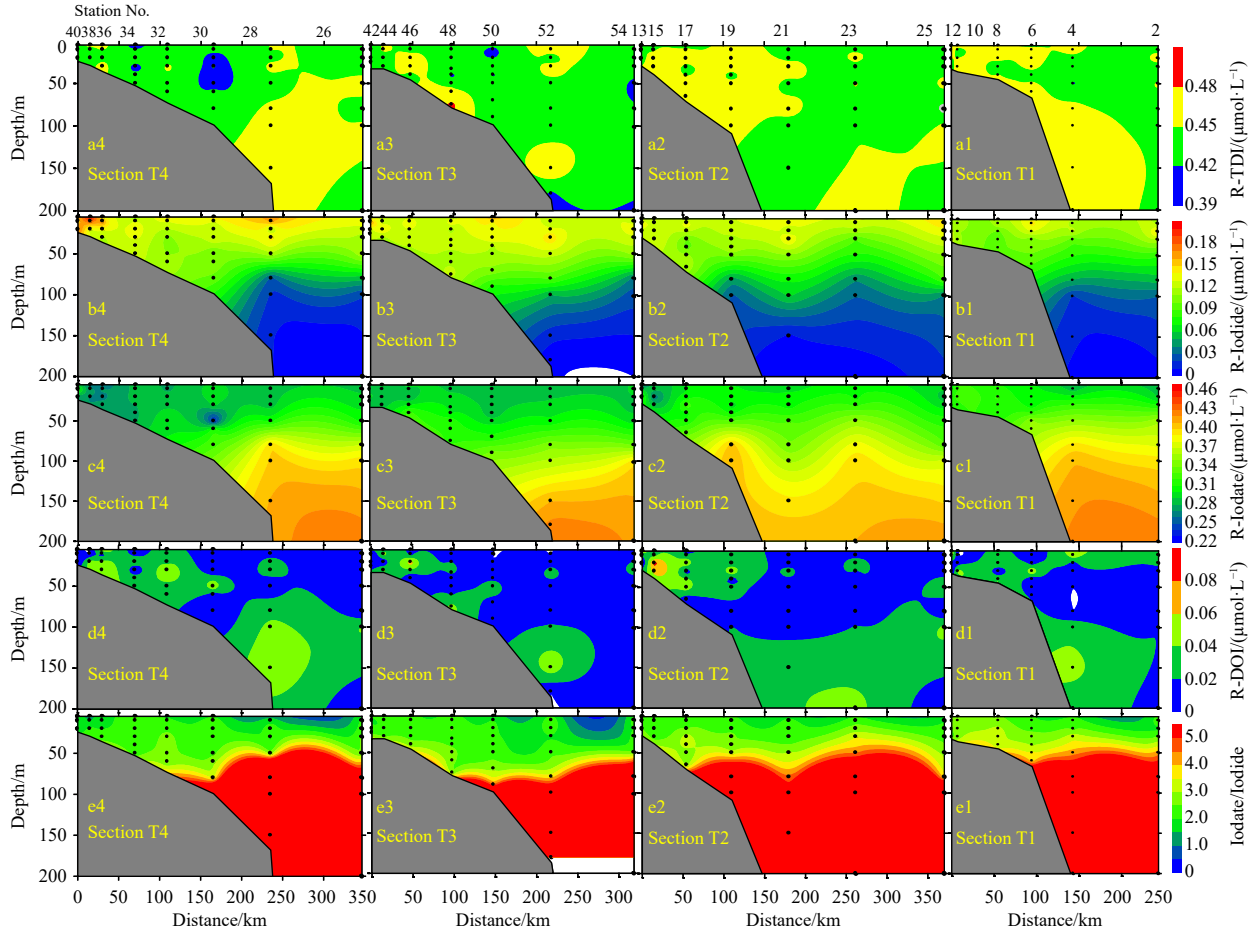

Fig. 6. Sectional distribution of R-Iodide, R-Iodate, R-DOI, and R-TDI and the iodate/iodide molar ratio in four sections in the cruise conducted in June 2010. R-*X* represents the normalized concentration to salinity 35.

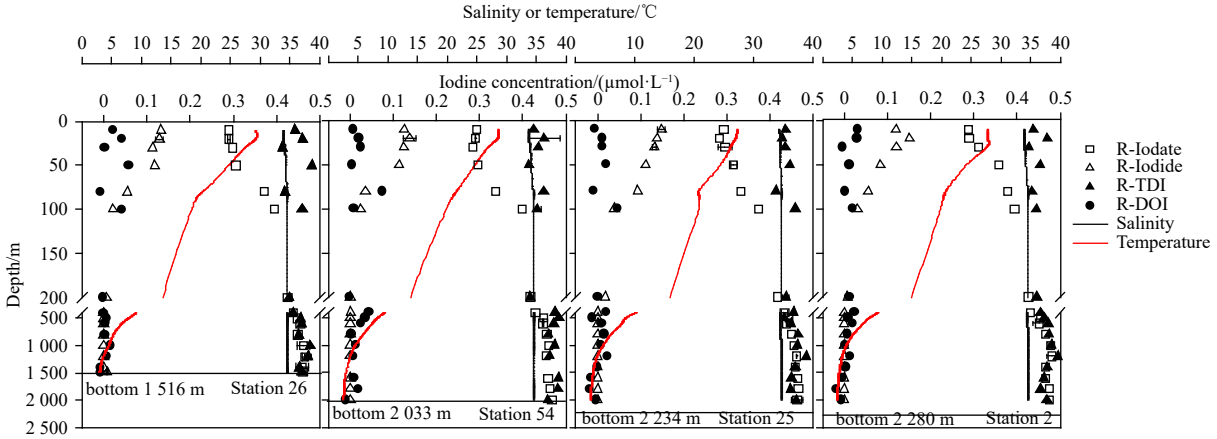

Fig. 7. Vertical distribution of R-Iodate, R-Iodide, R-DOI, and R-TDI in four stations during the cruise conducted in June 2010. R-*X* represents the concentration has been normalized to salinity 35.

ies and differences in iodine distribution between the South China Sea and the open ocean (To counteract the effects of physical changes, iodine is normalized to a salinity of 35).

Figure 8a shows that the relationship between IO_3^- and I^- in the South China Sea is not entirely in a 1:1 ratio. The data in the inner shelf show greater deviation, which may be due to the higher productivity of the inner shelf, where more iodine exist in the form of organic matter. The impact of river inputs may also be greater. The linear relationship between the iodate and iodide+DOI is found to be more in line with –1:1 (Fig. 8b). As a product of iodate, DOI cannot be neglected.

The relationship between R-TII and R-TDI (Fig. 9) also clearly illustrates the conversion relationship of iodine. R-TII represents all dissolved inorganic iodine, while R-TDI represents all dissolved iodine. If DOI can be ignored, the concentration of total inorganic iodine should be equivalent to the concentration of TDI. However, a significant difference is observed between the surface water of the inner and middle shelves. After taking into

Table 2. Average concentration of compositions in the mixed layer (0–40 m) and below (40–120 m) in the northern South China Sea Shelf conducted in June 2010

	Inner Shelf (0–40 m Ave.)		Mid-shelf (0–40 m Ave.)	Outer-shelf (0–40 m Ave.)	Open SCS (0–40 m Ave.)	SCS (0–40 m Ave.)
	Upwelling	Area (no upwelling)				
T/℃	24.417 ± 0.261	25.868 ± 1.152	25.686 ± 1.480	26.439 ± 1.368	25.899 ± 1.380	26.676 ± 1.344
S	34.221 ± 0.051	33.601 ± 0.767	34.027 ± 0.168	34.021 ± 0.206	33.929 ± 0.312	34.061 ± 0.252
IO_3^-/(μmol·L^{-1})	0.01 ± 0.02	0.85 ± 2.87	0.048 ± 0.107	0.006 ± 0.022	0.22 ± 0.71	0.06 ± 0.143
Chl a/(μg·L^{-1})	0.565 ± 0.191	0.733 ± 0.699	0.411 ± 0.299	0.195 ± 0.129	0.44 ± 0.35	0.304 ± 0.191
I^-/(μmol·L^{-1})	0.115 ± 0.007	0.131 ± 0.020	0.120 ± 0.015	0.127 ± 0.015	0.124 ± 0.016	0.123 ± 0.014
R-I^-/(μmol·L^{-1})	0.118 ± 0.007	0.138 ± 0.023	0.124 ± 0.016	0.131 ± 0.016	0.128 ± 0.017	0.127 ± 0.015
IO_3^-/(μmol·L^{-1})	0.306 ± 0.008	0.271 ± 0.018	0.287 ± 0.014	0.286 ± 0.011	0.283 ± 0.014	0.288 ± 0.011
R-IO_3^-/(μmol·L^{-1})	0.313 ± 0.008	0.283 ± 0.016	0.295 ± 0.013	0.294 ± 0.010	0.292 ± 0.015	0.296 ± 0.011
DOI/(μmol·L^{-1})	0.025 ± 0.027	0.025 ± 0.029	0.019 ± 0.022	0.015 ± 0.022	0.019 ± 0.024	0.014 ± 0.014
R-DOI/(μmol·L^{-1})	0.025 ± 0.027	0.025 ± 0.030	0.020 ± 0.023	0.016 ± 0.024	0.020 ± 0.024	0.014 ± 0.014
TDI/(μmol·L^{-1})	0.446 ± 0.019	0.427 ± 0.021	0.426 ± 0.023	0.428 ± 0.020	0.427 ± 0.022	0.424 ± 0.016
R-TDI/(μmol·L^{-1})	0.456 ± 0.020	0.447 ± 0.016	0.439 ± 0.023	0.442 ± 0.022	0.440 ± 0.023	0.437 ± 0.016
IO_3^-/I^-	2.7 ± 0.2	2.1 ± 0.3	2.6 ± 0.4	2.4 ± 0.4	2.5 ± 0.3	2.4 ± 0.4

	Mid-shelf (40–90 m Ave.)	Outer-shelf (40–90 m Ave.)	Shelf (0–120 m Ave.)	Open SCS (40–120 m Ave.)
T/℃	22.502 ± 1.106	20.590 ± 2.348	21.519 ± 1.744	20.734 ± 2.346
S	34.340 ± 0.130	34.494 ± 0.118	34.419 ± 0.124	34.498 ± 0.124
IO_3^-/(μmol·L^{-1})	1.27 ± 1.19	4.20 ± 4.10	2.74 ± 4.27	4.79 ± 3.30
Chl a/(μg·L^{-1})	0.557 ± 0.233	0.307 ± 0.199	0.432 ± 0.306	0.214 ± 0.128
I^-/(μmol·L^{-1})	0.111 ± 0.010	0.074 ± 0.036	0.093 ± 0.037	0.064 ± 0.032
R-I^-/(μmol·L^{-1})	0.113 ± 0.011	0.075 ± 0.037	0.095 ± 0.037	0.065 ± 0.033
IO_3^-/(μmol·L^{-1})	0.311 ± 0.024	0.342 ± 0.049	0.327 ± 0.055	0.351 ± 0.033
R-IO_3^-/(μmol·L^{-1})	0.318 ± 0.023	0.345 ± 0.048	0.332 ± 0.048	0.356 ± 0.032
DOI/(μmol·L^{-1})	0.025 ± 0.015	0.018 ± 0.018	0.022 ± 0.023	0.020 ± 0.021
R-DOI/(μmol·L^{-1})	0.026 ± 0.015	0.018 ± 0.018	0.022 ± 0.023	0.022 ± 0.022
TDI/(μmol·L^{-1})	0.447 ± 0.017	0.434 ± 0.021	0.441 ± 0.027	0.434 ± 0.019
R-TDI/(μmol·L^{-1})	0.456 ± 0.016	0.440 ± 0.020	0.448 ± 0.026	0.442 ± 0.020
IO_3^-/I^-	2.8 ± 0.4	7.1 ± 6.3	5.0 ± 6.3	7.6 ± 4.8

Note: Inner-shelf stations: 8, 10, 12, 13, 15, 36, 38, 40, 42, 44, 46. Upwelling stations: 10, 12. Mid-shelf stations: 6, 17, 32, 34, 48. Outer-shelf stations: 4, 19, 21, 28, 30, 42, 50. Open SCS stations: 2, 23, 26, 54.

account the error (the area between the two dashed lines is the range covered by the analysis error, with an error margin of ±0.02 μmol/L), it can be seen that some data with lower concentrations still fall outside the 1:1 relationship. Similarly, the deviation of the inner shelf is relatively large, which once again proves that although the DOI concentration is low, ignoring it will bring significant errors to the conversion products of iodate (Wong and Zhang, 2003a, 2003b).

4.3 *Iodine species output*

In general, iodate-rich and DOI-poor water from the open South China Sea intruded into the northern South China Sea shelf (Table 2), while iodide and DOI rich water was transported from the shelf into the open South China Sea. The reduction of iodate could have been carried out by the biologically mediated reduction (Bluhm et al., 2011; Moriyasu et al., 2020; MacKeown et al., 2022) or caused by natural light (Wong and Cheng, 2001a). In this study, a box model was applied to calculate the inter-conversion of the iodine species.

When water enters the continental shelf from the open sea area outside the shelf, the concentration of TDI remains basically unchanged while iodate decreases and iodide+DOI increases (Table 2). The conversion of iodate to iodide takes several months (Jickells et al., 1988; Wong, 1995). Iodide life can reach 1–20 years (Wong, 2001), while the half-life of DOI may only be a few hours (Wong and Cheng, 2001b). Nonetheless, there is a high possibility of recalcitrant DOI that resists degradation (Wong and Cheng, 1998), and the residence time of this part of the DOI is relatively long. There have been multiple reports on iodide transport (Wong, 1995; Wong and Zhang, 2003a; Wong et al., 2004; Wong and Cheng, 2008), yet DOI has not been reported.

Assuming that iodine on the northern shelf of the South China Sea is in a steady state, a box model is used to calculate the conversion and output of iodate, iodide, and DOI on the shelf (Fig. 10). According to the hydrological data, the upper mixed layer in the northern South China Sea during summer is about 40 m (Table 2), similar to the results in other studies (Cai et al., 2004; Wong et al., 2007).

The box model mainly considers the conversion of iodine species in the mixed layer of the northern shelf of the South China Sea (0–40 m). Its input and output include upwelling, advection input of the mixed layer outside the shelf (0–40 m), atmospheric deposition and river input, advection, and evaporation output of the mixed layer of the shelf (0–40 m) (Fig. 10).

For the South China Sea Shelf (0–40 m), the water flux is as follows:

$$F_R + F_P + F_V + F_{SH} = F_{HS} + F_E, \quad (1)$$

where F_R represents the water volume of the river, F_P represents wet deposition, F_V represents the water volume of upwelling, F_{SH} represents the water volume entering the shelf area outside the

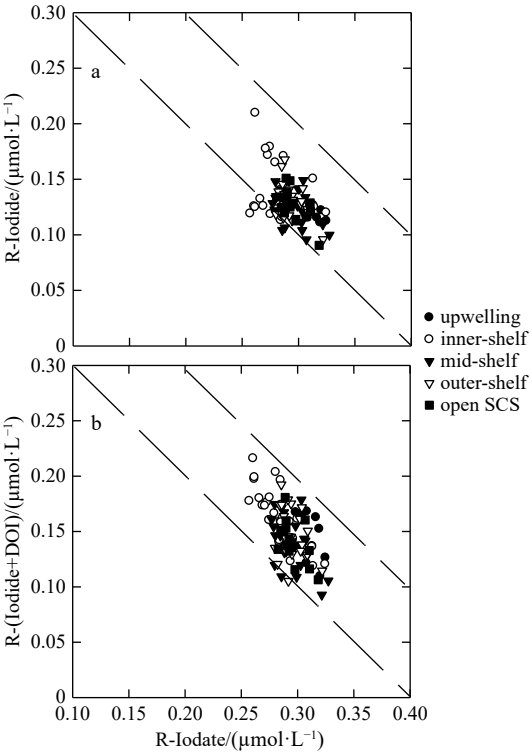

Fig. 8. Relationship between R-Iodate vs. R-Iodide (a) and R-Iodate vs. R-(Iodide+DOI) (b). The dashed lines represent the boundaries of the model-prescribed linear bands. R-*X* represents that the concentration has been normalized to salinity 35.

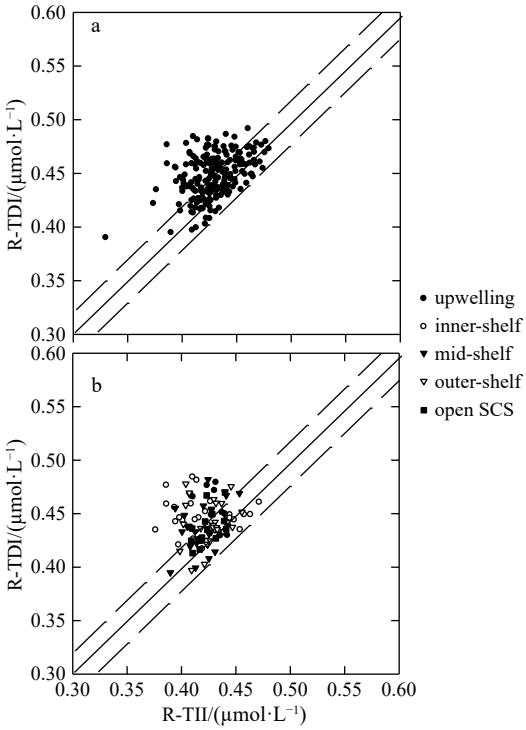

Fig. 9. Relationship between R-TII and R-TDI of all samples (a) or the samples from less than 40 m (b) in the cruise conducted in June 2010. The dashed lines represent the boundaries of the model-prescribed linear bands. R-*X* represents that the concentration has been normalized to salinity 35.

shelf, F_{HS} represents the water volume entering the shelf area from outside the shelf, and F_E represents the water volume evaporated from the shelf area.

In the model, input and output terms such as river inputs, evaporation, and subsidence on the northern shelf of the South China Sea can be ignored.

Equation (1) can be simplified as

$$F_V + F_{SH} = F_{HS}. \tag{2}$$

For the salt flux (S) on the South China Sea Shelf sea,

$$S_D F_V + S_S F_{SH} = F_{HS} S_H, \tag{3}$$

where S_D represents salt flux of upwelling, S_S represents salt flux of the mixed layer outside the shelf, and S_H represents salt flux of the mixed layer on the shelf.

The iodate, iodide, and DOI fluxes in the South China Sea Shelf sea are as follows:

$$A_D F_V + A_S F_{SH} = F_{HS} A_H + C_A \tag{4}$$

$$I_D F_V + I_S F_{SH} + P_I = F_{HS} I_H \tag{5}$$

$$O_D F_V + O_S F_{SH} + P_O = F_{HS} O_H \tag{6}$$

where A_D, I_D, and O_D represent the iodate, iodide, and DOI concentration in the upwelling; A_S, I_S, and O_S represent the three species' concentrations of the mixed layer outside the shelf; A_H, I_H, and O_H represent the concentrations of the mixed layer on the shelf sea; C_A is the iodate converted from the continental shelf; and P_I or P_O are the iodide or DOI converted from the continental shelf.

To distinguish the degree of influence of the inner, middle, and outer shelves on the conversion of iodine species, the shelves are divided into three parts (inner, middle, and outer parts). The parts outside the shelf area and the water volume of each part of the shelf were also calculated (Table 2). The weighted average concentration of each parameter (with water volume as the weight) was carried out for the mixed layer and below the mixed layer in each part, and the weighted average concentration and water volume of dissolved iodine in the mixed layer of the shelf were calculated separately. The results are listed in Table 3.

The volume of water in the whole shelf mixing layer is 8 074 km^3, residence time is 1.3 a, input (or output) volume of water is 6 210 km^3/a, and volume of shelf upwelling is 3 107 km^3, which accounts for about 50% of the annual input water (same as output). The annual input and output fluxes of salt are (210.7 ± 1.9) Pg and (212.6 ± 0.9) Pg, respectively. As the difference between them is (1.9 ± 2.0) Pg, it can still be considered as the basic balance of salt input and output.

To the shelf mixing layer, iodate input and output are 19.1 × 10^8 mol/a and 17.6 × 10^8 mol/a, respectively (Tables 3 and 4). The difference is 1.5 × 10^8 mol/a, which is about 8% of the total input iodate converted to iodide and DOI, far less than that of the East China Sea (~20%) and the U.S. coastal shelf (~28%). Furthermore, iodide input and output are 6.7 × 10^8 mol/a and 7.7 × 10^8 mol/a, respectively (Tables 3 and 4), and the difference is 1.00 × 10^8 mol/a. DOI input and output are 1.11 × 10^8 mol/a and 1.18 ×

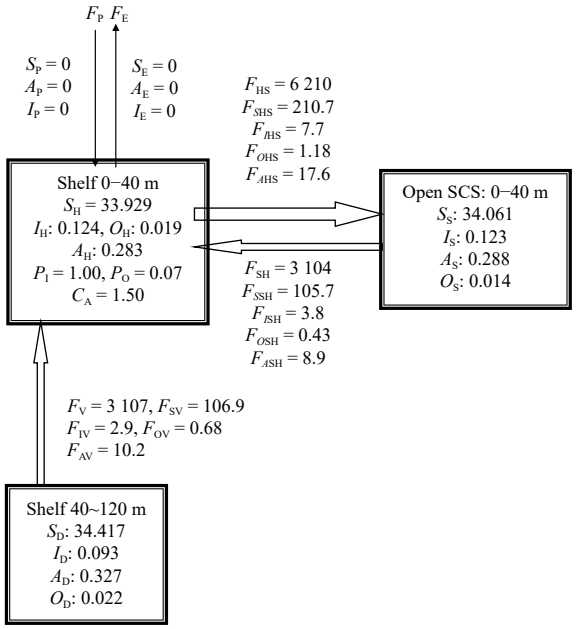

Fig. 10. Box model of iodine flux in the northern South China Sea Shelf. *F*, *S*, *A*, *I*, and *O* represent water flux (km³/a), salinity flux (10^{15} g/a), and the concentrations of iodate, iodide, and DOI (μmol/L), respectively. The subscripts R, H, D, S, P, and E represent river, shelf (0–40 m), shelf (40–120 m), open SCS (0–40 m), deposition, and evaporation fluxes, respectively. C_A, P_I, and P_O represent the consumption of iodate and the production of iodide and DOI in the shelf (10^8 mol/a).

10^8 mol/a, respectively (Tables 3 and 4), and the difference is 0.07×10^8 mol/a, hence, the total difference is 1.07×10^8 mol/a, indicating an increase of approximately 14%.

The model results show that iodate is mainly converted to iodide and a small fraction can be converted to DOI (Table 4), confirming that a portion of the net increase in DOI on the shelf can be exported.

The consumption rate of iodate on the northern shelf of the South China Sea is equivalent to 0.06 nmol/d, the production rate of iodide is equivalent to 0.04 nmol/d, and the production rate of DOI is 0.003 nmol/d. By comparison, in the East China Sea, the consumption rate of iodate is 0.10 nmol/d, and the production rate of iodide is 0.06 nmol/d (Wong et al., 2004). Therefore, the conversion efficiency of iodate may be higher in high-productivity marine areas. The annual average net primary productivity of the South China Sea and East China Sea shelf areas are 0.36 ± 0.15 g/(m²·a)(in terms of C) and 0.96 ± 0.38 g/(m²·a)(in terms of C), respectively(Gong et al., 2000; Lee Chen, 2005), where iodide and DOI are mainly produced by organisms. The production rate of iodide and consumption rate of iodate are approximately 5–6 nmol/d at South Atlantic Bight. The rates between different shelves can reach up to several tens of times. While the mechanism may be related to algal species, light intensity, or temperature, the exact mechanism still needs to be studied further.

5 Conclusions

TDI concentration is (0.43 ± 0.03) μmol/L and shows conservative behavior on the northern shelf of the South China Sea. The concentration range of iodide in the surface continental shelf is 0.11–0.20 μmol/L (~30% of TDI), following a pattern of near shore>far shore (not including upwelling). DOI concentration is 0–0.07 μmol/L (~10% of TDI, near shore>far shore).

Iodide concentration decreases with increasing depth and has dropped below 0.01 μmol/L by 200 m; on the contrary, iodate concentration increases with depth and reaches over 0.43 μmol/L at 200 m. Correspondingly, IO_3^-/I^- is 2.9 in the central area of the upwelling, gradually decreasing outward to 2.4. In other areas, the ratio is about 2, and the ratio can trace the upwelling scope.

The relationship between iodate and iodide is generally linear, with the slope slightly less than 1. This indicates that while DOI is only a small proportion, it should still not be neglected.

The results of the box model not only confirm that iodide pro-

Table 3. Average concentration of the compositions and fluxes in the box model in the northern South China Sea in June 2010

		Water		Salt		I^-		IO_3^-		DOI	
		Volume/ km³	Flux/ (km³·a⁻¹)	Salinity	Salt flux/ (10^5 g·a⁻¹)	Concentration/ (μmol·L⁻¹)	Flux/ (10^8 mol·a⁻¹)	Concentration/ (μmol·L⁻¹)	Flux/ (10^8 mol·a⁻¹)	Concentration/ (μmol·L⁻¹)	Flux/ (10^8 mol·a⁻¹)
Output	HS (0–40 m)	8 074	6 211	33.929 ± 0.312	210.7 ± 1.9	0.124 ± 0.016	7.70 ± 0.99	0.283 ± 0.014	17.57 ± 0.87	0.019 ± 0.024	1.18 ± 1.49
Input	Upwelling F_V (40–120 m)	3 107	3 107	34.417 ± 0.176	106.9 ± 0.5	0.093 ± 0.037	2.89 ± 1.15	0.327 ± 0.055	10.16 ± 1.71	0.022 ± 0.023	0.68 ± 0.72
	Advection SH (0–40 m)	–	3 104	34.061 ± 0.252	105.7 ± 0.8	0.123 ± 0.014	3.82 ± 0.43	0.288 ± 0.011	8.94 ± 0.34	0.014 ± 0.014	0.43 ± 0.43
	Total	–	6 211	–	212.6 ± 0.9	–	6.71 ± 1.23	–	19.10 ± 1.74	–	1.11 ± 0.84
Difference (Output–Input)		–	0	–	(–1.9) ± 2.0	–	0.99 ± 1.58	–	(–1.53) ± 1.95	–	0.07 ± 1.71

Note: – represents no data.

Table 4. Average concentration of the compositions and fluxes in the box model in the northern South China Sea in June 2010. Iodine input, output, and conversion ratio in the northern South China Sea.

	IO_3^-	I^-	DOI
Upwelling input/(10^8 mol·a⁻¹)	10.20	2.90	0.68
Translation input/(10^8 mol·a⁻¹)	8.90	3.80	0.43
Total input/(10^8 mol·a⁻¹)	19.10	6.70	1.11
Total output/(10^8 mol·a⁻¹)	17.60	7.70	1.18
Difference/(10^8 mol·a⁻¹)	1.50	1.00	0.07
Conversion rate/(nmol·d⁻¹)	0.06	0.04	0.003
Proportion/%	8	14	

Note: Upwelling input: flux input from 40 m to 90 m on the shelf to the mixed layer on the shelf; translation input: flux input from the continental slope to the mixed layer of the continental shelf.

duced can output but that DOI may also output. Iodate input to the shelf is approximately 19.10×10^8 mol/a, output is 17.60×10^8 mol/a, and amount of reduced iodate is 1.50×10^8 mol/a, accounting for approximately 8% of the total input. Meanwhile, the total flux of iodide and DOI input to the South China Sea shelf is 7.81×10^8 mol/a and the total output flux of iodide and DOI is 8.88×10^8 mol/a, showing an increased amount of 1.07×10^8 mol/a, which is 14% compared to the input.

This study aimed to investigate the iodine system in low-latitude marginal sea and active sites for iodine species conversion. However, compared to the mid-to-high-latitude marginal seas, the conversion efficiency of iodate is lower.

Acknowledgements

The author would like to thank MEL and RCEC for triggering this research and supplying the convenience of experiment, and the editors/anonymous reviewers for their insightful comments and suggestions.

References

Bluhm K, Croot P L, Huhn O, et al. 2011. Distribution of iodide and iodate in the Atlantic sector of the Southern Ocean during austral summer. Deep Sea Research Part II: Topical Studies in Oceanography, 58(25–26): 2733–2748, doi: 10.1016/j.dsr2.2011.02.002

Cai Weijun, Dai Minhan, Wang Yongchen, et al. 2004. The biogeochemistry of inorganic carbon and nutrients in the Pearl River estuary and the adjacent Northern South China Sea. Continental Shelf Research, 24(12): 1301–1319, doi: 10.1016/j.csr.2004.04.005

Callahan J, Dai Minhan, Chen R F, et al. 2004. Distribution of dissolved organic matter in the Pearl River Estuary, China. Marine Chemistry, 89(1–4): 211–224, doi: 10.1016/j.marchem.2004.02.013

Carrano M W, Yarimizu K, Gonzales J L, et al. 2020. The influence of marine algae on iodine speciation in the coastal ocean. Algae, 35(2): 167–176, doi: 10.4490/algae.2020.35.5.25

Chance R, Weston K, Baker A R, et al. 2010. Seasonal and interannual variation of dissolved iodine speciation at a coastal Antarctic site. Marine Chemistry, 118(3–4): 171–181, doi: 10.1016/j.marchem.2009.11.009

Dai Minhan, Wang Lifang, Guo Xianghui, et al. 2008. Nitrification and inorganic nitrogen distribution in a large perturbed river/estuarine system: the Pearl River Estuary, China. Biogeosciences, 5(5): 1227–1244, doi: 10.5194/bg-5-1227-2008

Gong Gwo-Ching, Shiah Fuh-Kwo, Liu Kon-Kee, et al. 2000. Spatial and temporal variation of chlorophyll *a*, primary productivity and chemical hydrography in the southern East China Sea. Continental Shelf Research, 20(4–5): 411–436, doi: 10.1016/S0278-4343(99)00079-5

Jickells T D, Boyd S S, Knap A H. 1988. Iodine cycling in the Sargasso Sea and the Bermuda inshore waters. Marine Chemistry, 24(1): 61–82, doi: 10.1016/0304-4203(88)90006-0

Lee Chen Yuh-Ling. 2005. Spatial and seasonal variations of nitrate-based new production and primary production in the South China Sea. Deep Sea Research Part I: Oceanographic Research Papers, 52(2): 319–340, doi: 10.1016/j.dsr.2004.11.001

Lin Jianrong. 2023. Dissolved iodine in the Changjiang River Estuary, China. Water Science and Technology, 88(5): 1269–1279, doi: 10.2166/wst.2023.263

MacKeown H, von Gunten U, Criquet J. 2022. Iodide sources in the aquatic environment and its fate during oxidative water treatment—A critical review. Water Research, 217: 118417, doi: 10.1016/j.watres.2022.118417

Moriyasu R, Evans N, Bolster K M, et al. 2020. The distribution and redox speciation of iodine in the eastern tropical North Pacific Ocean. Global Biogeochemical Cycles, 34(2): e2019GB006302, doi: 10.1029/2019GB006302

Pan Hailong, Gao Huiwang, Song Pingping, et al. 2006. Analysis of diffuse route of the Zhujiang River diluted water in summer. Marine Forecasts (in Chinese), 23(3): 58–63

Shaikh A, Kurian S, Shenoy D M, et al. 2023. Spatial and temporal variation of dissolved iodine in the eastern Arabian Sea. Marine Chemistry, 257: 104322, doi: 10.1016/j.marchem.2023.104322

Su Jilan. 2004. Overview of the South China Sea circulation and its influence on the coastal physical oceanography outside the Pearl River Estuary. Continental Shelf Research, 24(16): 1745–1760, doi: 10.1016/j.csr.2004.06.005

Truesdale, V. W. 1975. "Reactive" and "unreactive" iodine in seawater-a possible indication of an organically bound iodine fraction. Marine Chemistry, 3(2): 111–119, doi: 10.1016/0304-4203(75)90018-3

Truesdale V W. 1978. Iodine in inshore and off-shore marine waters. Marine Chemistry, 6(1): 1–13, doi: 10.1016/0304-4203(78)90002-6

Truesdale V W. 1994. Distribution of dissolved iodine in the Irish Sea, a temperate shelf sea. Estuarine, Coastal and Shelf Science, 38(5): 435–446

Truesdale V W, Danielssen D S, Waite T J. 2003. Summer and winter distributions of dissolved iodine in the Skagerrak. Estuarine, Coastal and Shelf Science, 57(4): 701–713

Truesdale V W, Jones K. 2000. Steady-state mixing of iodine in shelf seas off the British Isles. Continental Shelf Research, 20(14): 1889–1905, doi: 10.1016/S0278-4343(00)00050-9

Truesdale V W, Upstill-Goddard R. 2003. Dissolved iodate and total iodine along the British east coast. Estuarine, Coastal and Shelf Science, 56(2): 261–270

Tsunogai S, Henmi T. 1971. Iodine in the surface water of the ocean. Journal of Oceanography, 27(2): 67–72

Wong G T F. 1991. The marine geochemistry of Iodine. Reviews in Aquatic Sciences, 4(1): 45–73

Wong G T F. 1995. Dissolved iodine across the Gulf Stream Front and in the South Atlantic Bight. Deep Sea Research Part Ⅰ: Oceanographic Research Papers, 42(11–12): 2005–2023, doi: 10.1016/0967-0637(95)00087-9

Wong G T F. 2001. Coupling iodine speciation to primary, regenerated or "new" production: a re-evaluation. Deep Sea Research Part Ⅰ: Oceanographic Research Papers, 48(6): 1459–1476, doi: 10.1016/S0967-0637(00)00097-2

Wong G T F, Cheng Xianhao. 1998. Dissolved organic iodine in marine waters: Determination, occurrence and analytical implications. Marine Chemistry, 59(3–4): 271–281, doi: 10.1016/S0304-4203(97)00078-9

Wong G T F, Cheng Xianhao. 2001a. Dissolved organic iodine in marine waters: role in the estuarine geochemistry of iodine. Journal of Environmental Monitoring, 3(2): 257–263, doi: 10.1039/b007229j

Wong G T F, Cheng Xianhao. 2001b. The formation of iodide in inshore waters from the photochemical decomposition of dissolved organic iodine. Marine Chemistry, 74(1): 53–64, doi: 10.1016/S0304-4203(00)00095-5

Wong G T F, Cheng Xianhao. 2008. Dissolved inorganic and organic iodine in the Chesapeake Bay and adjacent Atlantic waters: Speciation changes through an estuarine system. Marine Chemistry, 111(3–4): 221–232, doi: 10.1016/j.marchem.2008.05.006

Wong G T F, Hung C C, Gong Gwo-Ching. 2004. Dissolved iodine species in the East China Sea—a complementary tracer for upwelling water on the shelf. Continental Shelf Research, 24(13–14): 1465–1484, doi: 10.1016/j.csr.2004.05.004

Wong G T F, Ku T L, Mulholland M, et al. 2007. The SouthEast Asian Time-series Study (SEATS) and the biogeochemistry of the South China Sea—An overview. Deep Sea Research Part Ⅱ: Topical Studies in Oceanography, 54(14–15): 1434–1447

Wong G T F, Zhang Lingsu. 1992. Changes in iodine speciation across coastal hydrographic fronts in southeastern United States continental shelf waters. Continental Shelf Research, 12(5–6): 717–733, doi: 10.1016/0278-4343(92)90027-H

Wong G T F, Zhang Lingsu. 2003a. Geochemical dynamics of iodine in marginal seas: the southern East China Sea. Deep Sea Research Part II: Topical Studies in Oceanography, 50(6–7): 1147–1162, doi: 10.1016/S0967-0645(03)00015-8

Wong G T F, Zhang Lingsu. 2003b. Seasonal variations in the speciation of dissolved iodine in the Chesapeake Bay. Estuarine, Coastal and Shelf Science, 56(5–6): 1093–1106

Wu Risheng, Li Li. 2003. Summarization of study on upwelling system in the South China Sea. Journal of Oceanography in Taiwan Strait (in Chinese), 22(2): 269–277

Yuan Liangying. 2005. Nutrient structure and its characteristics in the northern South China Sea (in Chinese). Master's Thesis. Research Center of Environmetal Science, Xiamen University, Xiamen.

Zhou Peng, Song Xiuxian, Yuan Yongquan, et al. 2017. Intrusion pattern of the Kuroshio Subsurface Water onto the East China Sea continental shelf traced by dissolved inorganic iodine species during the spring and autumn of 2014. Marine Chemistry, 196: 24–34, doi: 10.1016/j.marchem.2017.07.006